

# Granulosa cells regulate oocyte intracellular pH against acidosis in preantral follicles by multiple mechanisms

Greg FitzHarris<sup>1,2,\*</sup>, Violetta Siyanov<sup>1,3</sup> and Jay M. Baltz<sup>1,2,3</sup>

Mammalian oocytes grow within ovarian follicles in which the oocyte is coupled to surrounding granulosa cells by gap junctions. We report here that growing oocytes isolated from mouse preantral follicles are incapable of recovering from an experimentally induced acidosis, and that oocytes acquire the ability to manage acid loads by activating  $\text{Na}^+/\text{H}^+$  exchange during growth. By contrast, granulosa cells from similar preantral follicles possess substantial  $\text{Na}^+/\text{H}^+$  exchange capacity, which is attributable to the simultaneous action of two  $\text{Na}^+/\text{H}^+$  exchanger isoforms: NHE1 and NHE3. Granulosa cells were also found to possess a V-type  $\text{H}^+$ -ATPase that drives partial acidosis recovery when  $\text{Na}^+/\text{H}^+$  exchange is inactivated. By monitoring intracellular pH ( $\text{pH}_i$ ) in small follicle-enclosed oocytes, we found that the oocyte has access to each of these acidosis-correcting activities, such that small follicle-enclosed oocytes readily recover from acidosis in a manner resembling granulosa cells. However, follicle-enclosed oocytes are unable to access these activities if gap-junction communication within the follicle is inhibited. Together, these experiments identify the NHE isoforms involved in regulating oocyte  $\text{pH}_i$ , indicate that gap junctions allow granulosa cells to exogenously regulate oocyte  $\text{pH}_i$  against acidosis until the oocyte has acquired endogenous  $\text{pH}_i$  regulation, and reveal that granulosa cells possess multiple mechanisms for carrying out this function.

**KEY WORDS:**  $\text{Na}^+/\text{H}^+$  exchange, Granulosa cells, Oocyte, pH regulation

## INTRODUCTION

Regulation against unwelcome perturbations in intracellular pH ( $\text{pH}_i$ ) is a fundamental and essential process carried out by virtually all cells. The principal  $\text{pH}_i$  regulatory mechanisms in mammalian cells are  $\text{HCO}_3^-/\text{Cl}^-$  exchangers of the AE (anion exchange) family, which export  $\text{HCO}_3^-$  in exchange for  $\text{Cl}^-$  thereby correcting  $\text{pH}_i$  increases (Romero et al., 2004; Alper, 1994), and  $\text{Na}^+/\text{H}^+$  exchangers of the NHE (also known as *Scl9a* – Mouse Genome Informatics) gene family which correct  $\text{pH}_i$  decreases by exporting protons in exchange for  $\text{Na}^+$  (Orlowski and Grinstein, 1997; Orlowski and Grinstein, 2004). Multiple isoforms of the  $\text{Na}^+/\text{H}^+$  exchanger (NHE1–9) and the  $\text{HCO}_3^-/\text{Cl}^-$  exchanger (AE1–3, with numerous splice variants) exist, with heterogeneous tissue expression that probably reflects their different kinetic properties and regulation (Romero et al., 2004; Orlowski and Grinstein, 2004). These transport systems may be supplemented by additional components, such as  $\text{Na}^+$ ,  $\text{HCO}_3^-/\text{Cl}^-$  exchangers (NBC), which relieve acidosis in some cell types by importing  $\text{HCO}_3^-$  (Romero et al., 2004), and V-type  $\text{H}^+$ -ATPases (V-ATPases) which export protons across the plasmalemma in some cells (Nelson and Harvey, 1999; Merzendorfer et al., 1997; Kawasaki-Nishi et al., 2003). The multifaceted array of  $\text{pH}_i$  regulatory mechanisms provides the basis for tight control of intracellular pH in the face of external pH changes and metabolic acid generation. Perhaps unsurprisingly, impairment of  $\text{pH}_i$  regulation can compromise cell function and viability. For example, growth and proliferation is impaired in some  $\text{pH}_i$  regulation-compromised cells when intracellular  $\text{pH}_i$  is

disturbed (Grinstein et al., 1989; Kapus et al., 1994), and  $\text{pH}_i$  dysregulation jeopardizes cell survival (Pouyssegur et al., 1984).  $\text{pH}_i$  regulation is of particular importance in early mammalian development, as inhibition of  $\text{pH}_i$  regulatory mechanisms hinders preimplantation development in mouse and hamster embryos (Lane et al., 1998; Zhao et al., 1995).

Mammalian oocytes grow within ovarian follicles, discrete micro-organs consisting of the oocyte and a surrounding shell of (somatic) granulosa cells. Oocyte growth takes about 15 days in mouse, during which time the oocyte increases in diameter from about 15 to 70–80  $\mu\text{m}$ . Throughout growth, the oocyte remains coupled to its granulosa cells by gap junctions, intercellular channels that permit small molecules ( $<1$  kDa) to pass freely between apposing cells (Anderson and Albertini, 1976; Ducibella et al., 1975; Kidder and Mhaw, 2002). Growth of the oocyte is absolutely dependent upon its association with granulosa cells (Eppig, 1977; Eppig, 1979; Brower and Shultz, 1982; Eppig and Wigglesworth, 2000), and the importance of gap junction communication is well established, since oocyte growth is prevented by targeted deletion of gap junctions found within the follicle (Ackert et al., 2001; Simon et al., 1997). Gap junctions provide a means for granulosa cells to assist the oocyte in carrying out metabolic functions that the growing oocyte is not yet capable of. For example, granulosa cells promote oocyte uptake of some amino acids and nucleotides that are ineffectively taken up by denuded oocytes (Colonna and Mangia, 1983; Cross and Brinster, 1974; Haghighat and van Winkle, 1990; Heller et al., 1981; Heller and Schultz, 1980). In addition, although oocytes metabolise glucose poorly, granulosa cells metabolise glucose efficiently, and provide the oocyte with metabolic substrates that it can use (Biggers et al., 1967). However, although the ability of the granulosa cells to provide the oocyte with substrates is well established, there has been little evidence that granulosa cells assume homeostatic functions on behalf of the oocyte.

We recently showed that smaller growing oocytes isolated from the ovary with their granulosa cells removed ('denuded oocytes'), had a very limited ability to recover from an induced alkalosis,

<sup>1</sup>Ottawa Health Research Institute, <sup>2</sup>Department of Obstetrics and Gynecology (Division of Reproductive Medicine), and <sup>3</sup>Department of Cellular and Molecular Medicine, University of Ottawa, Ottawa, ON, K1Y 4E9, Canada.

\*Author for correspondence at present address: Institute for Women's Health, University College London, Gower Street, London WC1E 6BT, UK (e-mail: g.fitzharris@ucl.ac.uk)

whereas fully grown denuded oocytes recovered robustly (Erdogan et al., 2005). The ability to recover from alkalosis was acquired during oocyte growth as a result of activation of  $\text{HCO}_3^-/\text{Cl}^-$  exchange, which was inactive in very small oocytes ( $\sim 20\ \mu\text{m}$ ), showed only limited activity in denuded oocytes up to about  $60\ \mu\text{m}$  in diameter, and then became fully activated in oocytes when they were nearly fully grown ( $>65\ \mu\text{m}$ ) and competent to complete meiosis. Using an assay in which any  $\text{Na}^+/\text{H}^+$  exchanger activity could be revealed by an amiloride-sensitive intracellular acidification upon external  $\text{Na}^+$  removal, there was also evidence that  $\text{Na}^+/\text{H}^+$  exchanger activity follows a similar pattern during oocyte growth (Erdogan et al., 2005). Thus, we concluded that small growing oocytes do not possess intrinsic  $\text{pH}_i$  regulatory mechanisms, but develop them when they are nearly fully grown.

Subsequently it was found that, in the intact follicle, oocytes have access to significant amounts of alkalosis-correcting  $\text{HCO}_3^-/\text{Cl}^-$  exchange enabling them to recover from alkalosis, and that granulosa cells surrounding growing oocytes had substantial  $\text{HCO}_3^-/\text{Cl}^-$  exchange, which led us to propose that ovarian oocytes may be able to access  $\text{HCO}_3^-/\text{Cl}^-$  exchangers in the granulosa cells (FitzHarris and Baltz, 2006). However, it was difficult to discount the possibility that granulosa cells may activate  $\text{pH}_i$  regulation endogenous to the oocyte (FitzHarris and Baltz, 2006), and the lack of isoform-specific  $\text{HCO}_3^-/\text{Cl}^-$  exchange inhibitors prevented identification of the specific alkalosis-correcting mechanisms present in granulosa cells and fully grown oocytes.

The ability of growing oocytes to regulate against acidosis has not yet been addressed, nor have the molecular identities of any  $\text{pH}_i$ -regulatory mechanisms in oocytes or surrounding granulosa cells been determined. Our experiments described here indicate that growing oocytes rely upon granulosa cells to regulate against acidosis until the oocyte's own  $\text{Na}^+/\text{H}^+$  activity is activated during growth, and provide strong evidence that ooplasmic  $\text{pH}_i$  is regulated by  $\text{pH}_i$ -regulatory mechanisms within granulosa cells, which possess multiple mechanisms that can raise oocyte  $\text{pH}_i$ , including two  $\text{Na}^+/\text{H}^+$  exchanger isoforms and a proton-extruding V-ATPase, some of which are not present even in the fully grown oocyte.

## MATERIALS AND METHODS

### Chemicals and solutions

Chemicals and drugs were obtained from Sigma (St Louis, MO, USA) unless otherwise noted. Carboxysemaphthorhodafluor-1-acetoxymethyl ester (SNARF-1-AM), and SNARF-1-dextran were obtained from Molecular Probes (Eugene, OR, USA). Cariporide and S3226 were kindly supplied by Aventis. Stock solutions were prepared in either water [dibutyladenosine 3,5-cyclic monophosphate (dbcAMP)], ethanol (nigericin, NEM) or dimethyl sulfoxide (DMSO; SNARF-1-AM, valinomycin, DIDS, 1-octanol, 18 $\alpha$ -glycyrrhetic acid, cariporide, S3226, concanamycin).

All media were based on KSOM mouse embryo culture medium (Lawitts and Biggers, 1993) which contains (in mM) 95 NaCl, 2.5 KCl, 0.35  $\text{KH}_2\text{PO}_4$ , 0.2  $\text{MgSO}_4$ , 10 sodium lactate, 0.2 glucose, 0.2 sodium pyruvate, 25  $\text{NaHCO}_3$ , 1.7  $\text{CaCl}_2$ , 1 glutamine, 0.01 tetra sodium EDTA, 0.03 streptomycin sulphate and 0.16 penicillin G, and 1 mg/ml bovine serum albumin (BSA). Hepes-KSOM was used for oocyte collection and microinjection (21 mM Hepes replacing equimolar  $\text{NaHCO}_3$ , pH adjusted to 7.4). For fluorophore-loading and  $\text{pH}_i$  measurements, sodium lactate was reduced to 1 mM. Where used, bicarbonate-free medium was prepared by replacing  $\text{NaHCO}_3$  with equimolar NaCl. Experiments were performed in bicarbonate-containing medium unless otherwise stated. Nominally  $\text{Na}^+$ -free medium was prepared by replacing NaCl with equimolar choline chloride, and contained  $\sim 0.04\ \text{mM}\ \text{Na}^+$ . BSA were excluded from media during pH measurements to promote cellular adherence to the coverslip. The pH of all media were adjusted to 7.4 using NaOH or KOH.

### Oocyte and follicle handling, and microinjection

Oocytes and follicles were obtained from female CF1 mice (Charles River, St-Constant, PQ, Canada). Oocytes and follicles were isolated mechanically by fine mincing of the ovary with a razor blade, as previously described (Erdogan et al., 2005). A wave of follicular development occurs shortly after birth in mice, such that oocyte size and follicular development are related to postnatal age (Sorensen and Wassermann, 1976; Eppig, 1991), allowing recovery of growing oocytes and follicles of the required size by sacrificing mice of the appropriate age. Growing oocytes and pre-antral follicles were obtained from day 10 postnatal as described previously (FitzHarris and Baltz, 2006). Diameters of oocytes were determined from fluorescence images calibrated using a micrometer. At day 10, oocytes of  $40\text{--}60\ \mu\text{m}$  diameter were selected, and at day 20, oocytes of  $70\text{--}75\ \mu\text{m}$  were selected, representing the appropriate ranges for these neonates. Pre-antral follicles selected from day 10 mice had multiple layers of granulosa cells, and had not yet begun to form an antrum (secondary follicles). This population of follicles was  $\sim 95\text{--}115\ \mu\text{m}$  in diameter (oocyte plus surrounding granulosa cells). Where used, germinal vesicle-stage (GV) oocytes were obtained from primed adult female mice approximately 44 hours after equine chorionic gonadotropin injection as described previously (5 IU, intraperitoneally) (Philips et al., 2002).

Granulosa shells were prepared from pre-antral follicles of 10-day-old mice. Follicles were harvested following mincing of the ovary, as described above. Following a 30–60 minute incubation period, which rendered them less sticky, oocytes were removed from within the follicles by carefully applying pressure atop of the follicle with a glass micropipette. Only when the oocyte was observed to be expelled intact from the follicle, still enclosed in an unbroken zona pellucida, was the corresponding granulosa shell used for experiments. This could be accomplished for the majority of follicles. Though slightly more damaging to the structure of the granulosa shell than the oocyte removal method pioneered by Buccione and coworkers (Buccione et al., 1990), this method has the advantage that the oocyte remains intact when removed from the follicle, minimising contamination of the granulosa cells with ooplasm. *NHE4* mRNA, which always yielded a strong amplicon in denuded oocytes by RT-PCR (see Results), was not detected in granulosa shells, indicating that contamination of the shell by oocyte cytoplasm-derived material was minimal.

Oocyte microinjection was performed using a microinjection apparatus (Harvard Apparatus–Holliston, MA, USA) and micromanipulators (Narishige) mounted on a Zeiss Axiovert microscope, as previously detailed (FitzHarris and Baltz, 2006).

### Measurement of intracellular pH

$\text{pH}_i$  measurements were performed using a quantitative fluorescence imaging microscopy system (Inovision, Durham, NC, USA). pH was measured using SNARF-1 which was either microinjected in dextran-coupled form (SNARF-dex; 10 kDa, estimated final concentration  $0.5\text{--}1\ \text{mM}$ ), or loaded as the acetoxymethyl ester derivative (SNARF-AM  $5\ \mu\text{M}$ , 30 min), as previously described (FitzHarris and Baltz, 2006). SNARF was illuminated using 535 nm light, and emission monitored at 600 and 640 nm. The ratio of the two intensities (640/600) was calculated after background subtraction. Where shown, exemplar images are of the 640 nm emission. Calibration was performed using the nigericin/high  $\text{K}^+$  method with valinomycin added to collapse the  $\text{K}^+$  gradient (Baltz and Phillips, 1999).

### Ammonium pulse assay for monitoring recovery from acidosis

The ability of cells to manage acid loads was determined using the ammonium pulse assay, employed extensively in mammalian oocytes and embryos (Lane et al., 1998; Steeves et al., 2001; Harding et al., 2002). Cells were exposed to medium containing 35 mM  $\text{NH}_4\text{Cl}$  for 10 minutes. This  $\text{NH}_4\text{Cl}$  pulse initially causes an essentially instantaneous alkalosis as a result of rapid equilibration of  $\text{NH}_3$  across the plasma membrane. Subsequently, a more gradual  $\text{pH}_i$  decrease occurs as a result of much slower equilibration of  $\text{NH}_4^+$ . Upon removal of  $\text{NH}_4\text{Cl}$ ,  $\text{NH}_3$  exits the cell, leaving behind any  $\text{H}^+$  which initially entered the cell as  $\text{NH}_4$ , resulting in net intracellular acidification. In the present study, the 10-minute  $\text{NH}_4\text{Cl}$  pulse was followed immediately in all cases by a 10 minute exposure to  $\text{NH}_4\text{Cl}$ -free,  $\text{Na}^+$ -free medium, which allows the  $\text{Na}^+$ -dependence of acidosis correction to be established.

### Detection of mRNAs in oocytes and granulosa cells using RT-PCR

RNA extraction was performed using an RNeasy Micro kit (Qiagen), and reverse transcription performed using a Retroscript kit (Ambion), according to manufacturers' instructions. RNA extraction and reverse transcription were performed upon groups of no fewer than 60 oocytes or between eight and 25 granulosa shells at a time. PCR was performed using HotStarTaq PCR kit (Qiagen) on an appropriate amount of cDNA template corresponding to three oocytes, or one granulosa shell. Kidney (*NHE1-4*) and brain (*NHE5*) cDNA were used as positive controls. The amount of positive control tissue cDNA used was chosen to approximately correspond with that of three oocytes based upon measurement of RNA content of control tissue RNA preparations, and the known RNA content of one oocyte (~0.6 ng) (Sternlicht and Schultz, 1981). The same amount of positive control cDNA was used for comparison with granulosa shells, one granulosa shell having approximately the same volume as three fully grown oocytes. Samples of the final drops of medium in which oocytes were washed were subjected to the same reverse transcription protocol and used as negative controls. PCR was repeated on a minimum of two different oocyte preparations, or three different granulosa cell preparations. Amplicons were visualized on a 1% agarose gel containing 0.13 µg/ml ethidium bromide. All products were of the predicted size according to their position on the gel, and the identities of products from all five primer pairs were confirmed by direct sequencing.

Primers used for PCR were as follows (5'-3') [accession number; predicted amplicon length]. *NHE1* (also known as *Sc19a1*): CACCAGTGGAACTGGACCTT, AAGGTGGTCCAGGAAGTGTG [NM\_016981.1; 372]. *NHE2* (*Sc19a2*): ATCACGGCTGCTATTGTCGTT, GTGACCC-CAGTGTCCACACACA [NM\_001033289; 189]. *NHE3* (*Sc19a3*): TCAGCTAAGCTAGGCATCAACC, ATGGTGTTCAGGCGGCGGAAGT [AK033564; 412]. *NHE4* (*Sc19a4*): CCGGAGGAACCTGCCAAAATC, TCTTCAGGAGAAAGCCGCTTGA [NM\_177084; 162]. *NHE5* (*Sc19a5*): CCTCCCTGTTGTGGTCAGT, TATGGGAGATGTTGGCT-TCC [NM\_138858; 235]. Primers for *NHE1-4* were designed based upon

mouse mRNA sequences. Primers for *NHE5* were generated by 'blasting' the sequence for rat *NHE5* mRNA (NM\_138858) against the mouse genome. Primers were then designed using the matching mouse sequence. PCR products were sequenced and similarity to predicted sequences were as follows: *NHE1* 98%; *NHE2* 97%; *NHE3* 100%; *NHE4* 96%; *NHE5* 95%.

### Data analysis

Where rates of  $pH_i$  change were calculated, individual oocytes and/or granulosa shells within a given replicate were pooled to provide an average rate, and the mean±s.e.m. of the different replicates presented. Rates were calculated using SigmaPlot 8.0. Data points presented are the mean±s.e.m. of all replicates performed. Means of replicates were compared using *t*-tests (two groups) or ANOVA (three or more groups). Where ANOVA was used, Tukey-Kramer's and Dunnnett's post-hoc tests were applied as appropriate (using Instat; GraphPad, San Diego, CA, USA).

## RESULTS

### Oocytes acquire the capacity to recover from acidosis during growth by activating $Na^+/H^+$ exchange

We first set out to determine whether denuded growing oocytes are capable of recovering from acidosis. Two separate populations were examined; fully grown oocytes (70-75 µm in diameter) obtained from 20-day-old mice, and smaller, mid-growth-phase oocytes (40-60 µm) obtained from 10-day-old mice (see Materials and methods). Oocytes were freed of their granulosa cells, and loaded with the pH-sensitive fluorophore SNARF. Acidosis was induced by exposing oocytes to a 10 minute pulse of 25 mM  $NH_4Cl$  ( $NH_4Cl$  pulse assay; see Materials and methods for detailed explanation). This protocol caused substantial net acidosis in oocytes of all sizes (~0.5 pHU; Fig. 1).

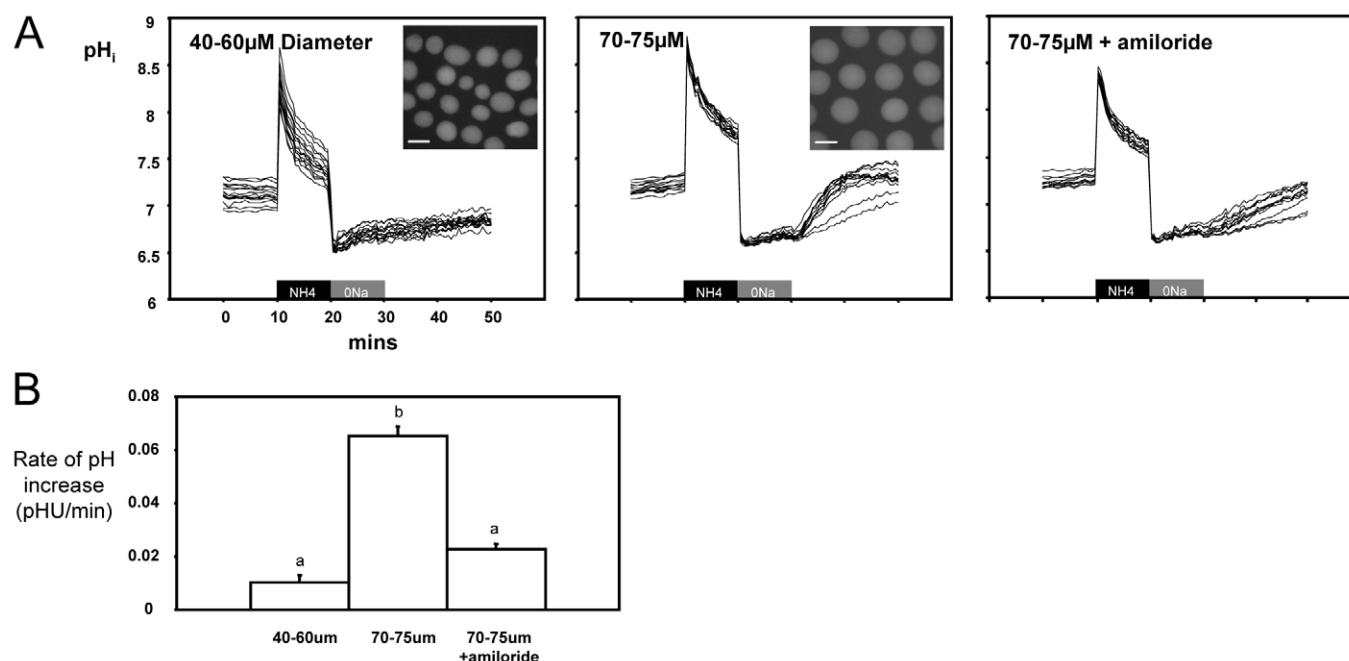


**Fig. 1. Activation of  $Na^+/H^+$  exchange during oocyte growth.** Intracellular pH was monitored in growing oocytes using epifluorescence microscopy. **(A)** Each panel shows a typical replicate of a given experiment, each individual trace representing a single oocyte. Acidosis was induced in mid-growth phase (left panel) and fully grown (middle panel) oocytes using a 10-minute pulse of  $NH_4Cl$  (black bar). Note that neither population of oocytes mounts a substantial recovery from acidosis in media devoid of  $Na^+$  (gray bar), but resting pH is rapidly restored in fully grown oocytes following  $Na^+$  replacement. Insets show exemplar fluorescence micrographs from each respective experiment. Scale bar: 50 µm. Where used, amiloride (1 mM) was added at  $t=20$  minutes, and remained in the bath thereafter. Note that amiloride retards recovery from acidosis in fully grown oocytes (right panel). **(B)** Analysis of rate of recovery from acidosis following  $Na^+$  replacement. Different letters above the bars indicate significant differences  $P<0.01$  (ANOVA). Three replicates were performed of each experiment – a total of 52, 32 and 39 oocytes, respectively.



There was minimal recovery from the induced acidosis in the subsequent 10 minute period during which  $\text{Na}^+$  was absent from the bathing medium. Replacement of  $\text{Na}^+$  caused a rapid  $\text{pH}_i$  increase in fully grown oocytes (initial rate of recovery  $0.065 \pm 0.003$  pHU/minute), the majority (78%) fully recovering from acidosis within 10 minutes. In sharp contrast, little or no recovery from acidosis was made by mid-growth oocytes ( $0.010 \pm 0.002$  pHU/minute; Fig. 1). To determine whether  $\text{Na}^+/\text{H}^+$  exchange may account for the  $\text{Na}^+$ -dependent recovery from acidosis in fully grown oocytes, acidosis was induced in the presence of amiloride, a broad-spectrum inhibitor of  $\text{Na}^+/\text{H}^+$  exchangers. Amiloride caused a substantial and highly significant inhibition of acidosis recovery (initial recovery rate  $0.023 \pm 0.004$  pHU/minute;  $P < 0.002$ ), although there was also a small amiloride-insensitive component of recovery (Fig. 1C). Oocytes thus acquire the ability to regulate against acidosis during growth by activating mechanisms which raise  $\text{pH}_i$ , of which  $\text{Na}^+/\text{H}^+$  exchange is the dominant component.

### Characterization of $\text{Na}^+/\text{H}^+$ exchange in fully grown oocytes

We next sought to determine the molecular identity of the  $\text{Na}^+/\text{H}^+$  exchanger(s) which alleviate acidosis in fully grown denuded oocytes. At least nine isoforms of the  $\text{Na}^+/\text{H}^+$  exchanger exist (NHE1-9), five of which (NHE1-5) are known to reside in the plasmalemma and may therefore participate in cytoplasmic  $\text{pH}_i$  regulation (Orlowski and Grinstein, 2004; Nakamura et al., 2005). We first carried out RT-PCR to determine which of these isoforms are present in oocytes at the mRNA level. Primers were designed to specifically amplify cDNA generated from *NHE1-5*. All five primer sets generated distinct amplicons of the predicted size from positive control cDNA, and no amplicons were detected in negative controls. Amplicons of the predicted sizes were always detected for *NHE1*, *NHE3* and *NHE4*, but not *NHE2* or *NHE5*, both in oocytes from day 20 mice (fully grown oocytes) and in oocytes from day 10 mice (mid-growth phase oocytes; Fig. 2A).

We next wanted to take a functional approach to determine which NHE isoform(s) regulates against acidosis in denuded oocytes. Although specific inhibitors of  $\text{HCO}_3^-/\text{Cl}^-$  (AE) and  $\text{Na}^+ \text{HCO}_3^-/\text{Cl}^-$  (NBC) exchangers remain elusive, a number of amiloride derivatives with isoform-selectivity for NHEs are available (Masereel et al., 2003). Since our previous experiment revealed a small amiloride-insensitive component of  $\text{pH}_i$  recovery in fully grown denuded oocytes, we carried out this further characterization of  $\text{Na}^+/\text{H}^+$ -exchange-mediated acidosis correction in  $\text{HCO}_3^-$ -free medium to inactivate  $\text{Na}^+ \text{HCO}_3^-/\text{Cl}^-$  exchange, which may account for the amiloride-insensitive component. As in bicarbonate-containing medium, only large oocytes made a significant recovery from acidosis following  $\text{NH}_4\text{Cl}$  exposure (Fig. 2B). Variation of recovery rates between oocytes within a given experiment was accentuated in bicarbonate-free medium, with a number of oocytes (31%) failing to recover from acidosis within each experiment. Nonetheless, the majority of oocytes (69%) recovered fully within 20 minutes, and the average rate of recovery was not significantly less than in bicarbonate-containing medium ( $0.056 \pm 0.02$  pHU/minute;  $P > 0.1$ ). Recovery was completely inhibited by amiloride in  $\text{HCO}_3^-$ -free conditions, consistent with the notion that the small amiloride-insensitive component seen in the presence of  $\text{HCO}_3^-$  might be  $\text{Na}^+ \text{HCO}_3^-/\text{Cl}^-$  exchange (Fig. 2B).

Next, to identify the origin of  $\text{Na}^+/\text{H}^+$  exchange activity, two isoform-selective  $\text{Na}^+/\text{H}^+$ -exchange inhibitors were employed. Cariporide (HOE 642) is a highly specific NHE1 inhibitor with published  $\text{IC}_{50}$ s in the region of 0.3–3.0  $\mu\text{M}$ , which has been used to

identify NHE1-dependent  $\text{pH}_i$  regulation in a variety of cell types (Masereel et al., 2003). S3226 exhibits a high level of selectivity for NHE3 at low concentrations ( $\text{IC}_{50}$ s 0.02–0.7  $\mu\text{M}$ ), and at higher concentrations also inhibits NHE1 ( $\text{IC}_{50}$ s  $\sim 3$   $\mu\text{M}$ ) (Schwark et al., 1998). Both drugs are well characterized, and their effective range in various cell types has been extensively reported (Schwark et al., 1998; Masereel et al., 2003). They have only been used previously in early mouse embryos to attempt to distinguish NHE isoforms responsible for  $\text{Na}^+$  transport necessary for blastocyst formation (Kawagishi et al., 2004).

Here, cariporide potently inhibited the  $\text{Na}^+$ -dependent recovery from acidosis in fully grown denuded oocytes, with substantial inhibition achieved at 1  $\mu\text{M}$ , indicating that inhibition of NHE1 is sufficient to prevent acidosis recovery (Fig. 2C,D). Complete inhibition was also achieved by 10  $\mu\text{M}$  S3226, which would be expected to inhibit both NHE1 and NHE3. However, 0.1  $\mu\text{M}$  S3226 had no effect (Fig. 2C,D). These experiments indicate that recovery from acidosis in fully grown denuded oocytes occurs principally via NHE1.

### Recovery from acidosis in granulosa cells from pre-antral follicles

Previously, it was found that small growing oocytes are only capable of recovering from an induced alkalosis when they remain within the follicle. Since granulosa cells have robust  $\text{HCO}_3^-/\text{Cl}^-$  exchange, we proposed that gap junctions may allow the granulosa cells to regulate the pH of the ooplasm (FitzHarris and Baltz, 2006). We therefore wanted to determine whether granulosa cells also possess significant acidosis-correcting capacity which might be able to control oocyte  $\text{pH}_i$  in the acid range. To address this, intact shells of granulosa cells were prepared by removing the oocyte from preantral follicles collected from 10-day-old mice (Fig. 3A; see Materials and methods for details). Granulosa shells were loaded with SNARF, and recovery from acidosis monitored using the  $\text{NH}_4\text{Cl}$ -pulse approach, as for oocytes.  $\text{NH}_4\text{Cl}$  treatment resulted in substantial net acidosis, as in oocytes (Fig. 3B).  $\text{Na}^+$  replacement triggered a rapid recovery from acidosis in all cases ( $0.064 \pm 0.011$  pHU/minute), which was substantially inhibited by amiloride (initial rate of recovery 0.023 pHU/minute;  $P < 0.05$ ; Fig. 3B,C). Thus, granulosa cells possess robust  $\text{Na}^+/\text{H}^+$  exchange which is their dominant means of correcting acidosis.

### Characterization of granulosa cell $\text{Na}^+/\text{H}^+$ exchange

Next, RT-PCR was carried out to establish which NHE mRNAs are expressed in granulosa shells. Distinct amplicons were produced by primers on all occasions only by *NHE1* and *NHE3* (Fig. 4A). Cariporide and S3226 were then used to determine which NHE isoforms are responsible for the  $\text{Na}^+$ -dependent, amiloride-sensitive recovery from acidosis in granulosa cells. As for oocytes, characterization of  $\text{Na}^+/\text{H}^+$  exchange was carried out in  $\text{HCO}_3^-$ -free medium to inhibit any  $\text{Na}^+$ -dependent  $\text{HCO}_3^-/\text{Cl}^-$  exchange which may be present. Somewhat unexpectedly, under these conditions there was always a slow but steady recovery from acidosis in the absence of  $\text{Na}^+$  ( $0.0233 \pm 0.004$  pHU/minute; Fig. 4B,C). Nevertheless,  $\text{pH}_i$  increased very rapidly when  $\text{Na}^+$  was replaced ( $0.085 \pm 0.009$  pHU/minute), such that the  $\text{Na}^+$ -dependent component could easily be determined (Fig. 4B). As expected, the  $\text{Na}^+$ -dependent component was inhibited by amiloride, confirming  $\text{Na}^+/\text{H}^+$  exchange (Fig. 4B). However, neither 1  $\mu\text{M}$  nor 10  $\mu\text{M}$  cariporide inhibited the  $\text{Na}^+$ -dependent component (Fig. 4C,D). By contrast, whereas 1  $\mu\text{M}$  S3226 had no effect, recovery was

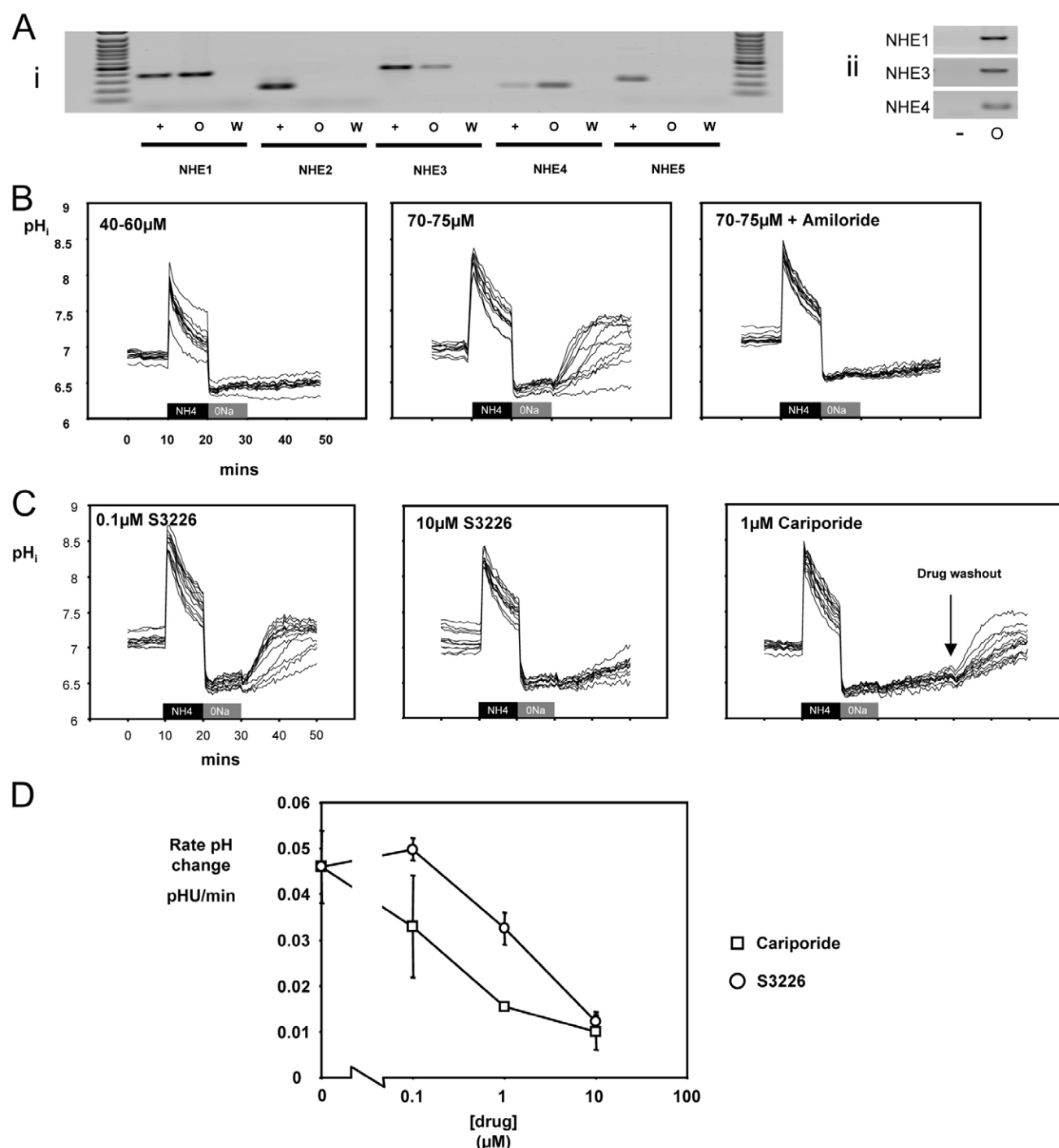


**Fig. 2. Identification of NHE isoforms that correct acidosis in fully grown oocytes.** (Ai) RT-PCR of NHE isoforms in fully grown oocytes from 20-day-old mice. Amplicons formed by reverse transcription and PCR of positive control tissues (+), three oocyte equivalents (O), or the final oocyte wash drop (–) are shown for each isoform, as indicated. For further details see Materials and methods. DNA ladder is in 100 bp increments. Distinct amplicons were always generated from oocyte samples by *NHE1*, *NHE3* and *NHE4* primers, but were never by *NHE5* primers, and a very faint band was produced by *NHE2* primers using 40 cycles of PCR in four of nine replicates. (Aii) RT-PCR of denuded oocytes from day-10 mice. Note that distinct amplicons were generated by primers for *NHE1*, *NHE3* and *NHE4*. Amplicons were not generated by primers for *NHE2* or *NHE5* (not shown). (B) Recovery from acidosis in mid-growth phase and fully grown oocytes in bicarbonate-free medium. Note that, as was also the case in the presence of bicarbonate (see Fig. 1), only fully grown oocytes recover from acidosis. (C) Typical examples of NH<sub>4</sub>Cl pulse experiments on fully grown oocytes in bicarbonate-free media in the presence of cariporide and S3226, as indicated. In each case, the drug was added at *t*=20 minutes, and remained throughout the experiment unless otherwise indicated. Note that 1 μM cariporide completely and reversibly inhibited acidosis recovery. (D) Summary of all experiments performed in this series plotted on a logarithmic scale. Drugs were diluted in DMSO such that the final concentration of DMSO was 0.1% throughout. Note the break in the x-axis to allow inclusion of a drug-free group (DMSO only). DMSO alone did not influence the rate of recovery (*P*>0.5). Each data point represents mean±s.d. of the initial rate of pH recovery from three separate replicates, comprising between 41 and 26 oocytes.

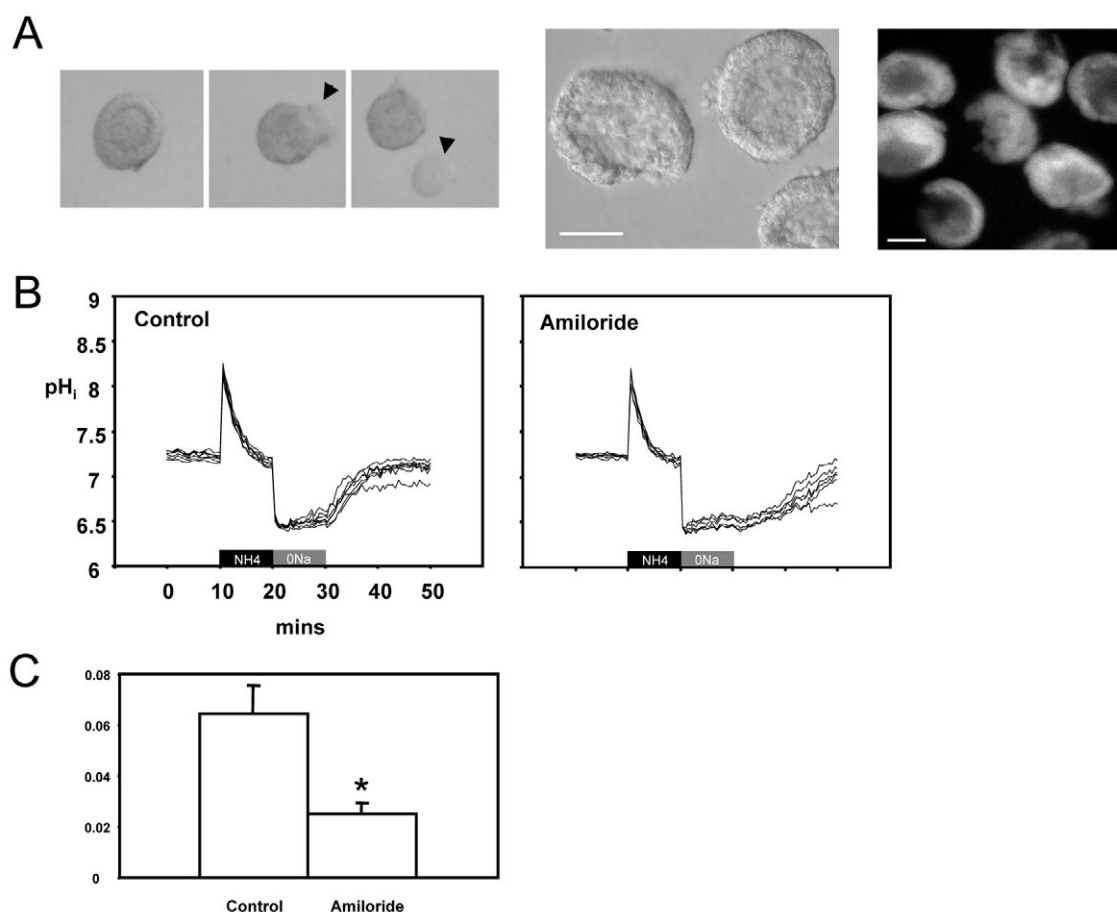


**Fig. 3. Recovery from acidosis in isolated granulosa cells.** Granulosa shells were prepared by removing the oocyte from preantral follicles recovered from 10-day-old mice, and then loaded with SNARF-AM. **(A)** Left, a series of three photomicrographs illustrating the procedure by which the oocyte (arrowheads) is removed from a preantral follicle. A higher resolution exemplar photomicrograph of the resulting granulosa shell is also shown (center) and a fluorescence micrograph of SNARF-loaded shells (right). Scale bar: 50  $\mu\text{m}$ . **(B)** Recovery from acidosis in SNARF-loaded granulosa shells following a  $\text{NH}_4\text{Cl}$  pulse. Note the rapid increase in pH when  $\text{Na}^+$  was returned to the bath (experiments were performed in triplicate,  $n=23$  in total). Note also that amiloride retarded  $\text{Na}^+$ -dependent acidosis correction (experiments were performed in triplicate,  $n=23$  in total). Amiloride was added at  $t=10$  minutes. **(C)** Average rate of recovery from acidosis following  $\text{Na}^+$  replacement. \*,  $P < 0.05$ .

substantially inhibited by 10  $\mu\text{M}$  S3226 (Fig. 4C,D). Given the previously reported  $\text{IC}_{50}$ s of S3226 for NHE1 and NHE3, we reasoned that the ability of 10  $\mu\text{M}$  S3226 (but not 1  $\mu\text{M}$  S3226 or 10  $\mu\text{M}$  cariporide) to prevent acidosis recovery in granulosa cells may be due to simultaneous activities of NHE1 and NHE3 that are both inhibited at high S3226 concentration. To test this possibility, we performed  $\text{NH}_4\text{Cl}$ -pulse experiments in the simultaneous presence of 10  $\mu\text{M}$  cariporide and 1  $\mu\text{M}$  S3226, treatments expected to inhibit NHE1 and NHE3, respectively, but which individually had no effect upon granulosa cells. This cariporide-S3226 co-treatment inhibited acidosis recovery to a similar degree as amiloride or 10  $\mu\text{M}$  S3226 (Fig. 4C,D). Therefore, recovery from acidosis in granulosa cells is inhibited by amiloride, 10  $\mu\text{M}$  S3226, or 1  $\mu\text{M}$  S3226 + 10  $\mu\text{M}$  cariporide, all of which are expected to block both NHE1 and NHE3 simultaneously. On the contrary, granulosa cells remain capable of recovering from acidosis if only one isoform is inhibited.

#### Characterization of $\text{Na}^+$ -independent recovery from acidosis in granulosa cells

We next wanted to identify the  $\text{Na}^+$ -independent means of acidosis recovery which was evident in granulosa cells in  $\text{HCO}_3^-$  free medium. This mechanism was uninhibited by any of the NHE

inhibitors (see Fig. 4B,C). In experiments in which  $\text{Na}^+$  was not returned to the medium, granulosa cell pH recovered almost fully within 20 minutes of  $\text{NH}_4\text{Cl}$  removal ( $78 \pm 4\%$  recovery; Fig. 5A). One possibility was that this slow  $\text{pH}_i$  increase may be attributable to a V-type  $\text{H}^+$ -ATPase, which are commonly found on intracellular membranes, but have been found on plasmalemmae and shown to correct acidosis in  $\text{Na}^+$ - and  $\text{HCO}_3^-$ -free conditions in some cells (Merzendorfer et al., 1997; Kawasaki-Nishi et al., 2003). *N*-ethylmaleimide (NEM; 100  $\mu\text{M}$ ), a widely employed nonspecific inhibitor of V-ATPases, abolished the  $\text{Na}^+$ -independent recovery from acidosis (initial rate of recovery  $0.001 \pm 0.003$  pHU/minute compared with controls  $0.023 \pm 0.004$  pHU/minute;  $P < 0.01$ ; Fig. 5A). However, subsequent re-addition of  $\text{Na}^+$  did not trigger a  $\text{pH}_i$  increase in these experiments, implying that  $\text{Na}^+/\text{H}^+$  exchange was also incapacitated by NEM (Fig. 5A). Though  $\text{Na}^+/\text{H}^+$  exchange is clearly not responsible for the  $\text{Na}^+$ -independent pH increase, this result raises questions about the specificity of NEM in these experiments. We therefore also employed bafilomycin and concanamycin, two related macrolide antibiotics that are highly specific for V-ATPases (Bowman et al., 1988; Drose and Altendorf, 1997). Inhibition of proton transport by nanomolar concentrations of concanamycin or bafilomycin is a strong indication of a role for

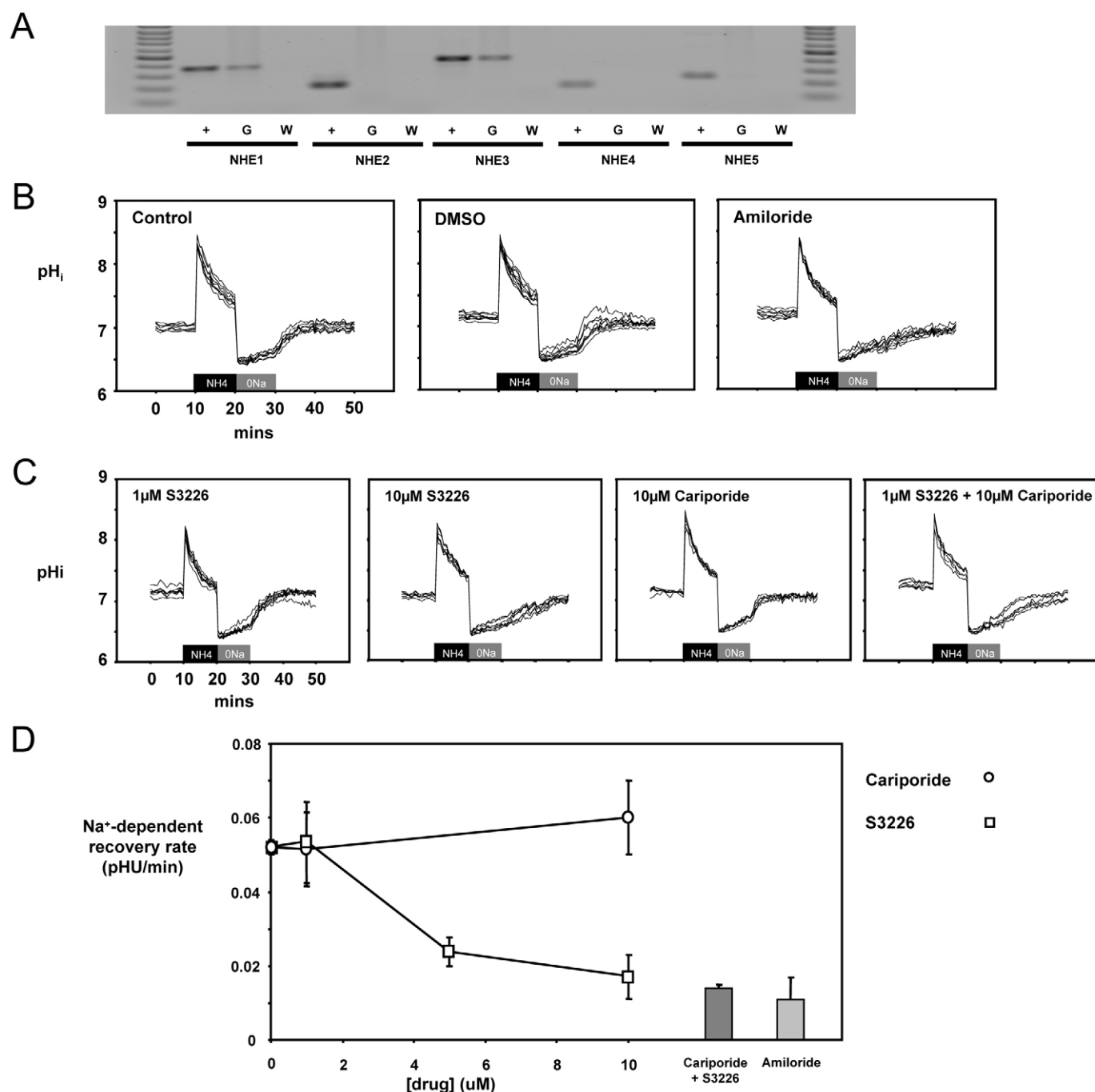


**Fig. 4. Identification of NHE isoforms that correct acidosis in granulosa shells.** (A) RT-PCR of NHE isoforms in granulosa shells isolated from 10-day-old mice. For each isoform, products formed by reverse transcription and PCR of positive control tissues (+), one follicle-equivalent of granulosa cells (G), or oocyte bathing media (–) are shown. For further details see Materials and methods. (B) Acidosis recovery in granulosa cells in bicarbonate-free medium. Note that amiloride retards the Na<sup>+</sup>-dependent pH<sub>i</sub> increase that occurs under control conditions. (C) Examples of NH<sub>4</sub>Cl pulse experiments of granulosa shells in bicarbonate-free medium in the presence of cariporide and S3226 (as indicated in each panel). In each case, the drug was added at *t*=10 minutes, and remained throughout the experiment. (D) Summary of all experiments performed in this series. DMSO (vehicle) was 0.1% throughout. DMSO alone had no effect upon acidosis recovery. Since some recovery occurs during the Na<sup>+</sup>-free period in granulosa cells in these experiments, the rate of pH<sub>i</sub> increase during the Na<sup>+</sup>-free period was subtracted to obtain the Na<sup>+</sup>-dependent component of recovery. Each data point represents mean ± s.d. of the Na<sup>+</sup>-dependent pH<sub>i</sub> recovery from three to five separate replicates, comprising between 18 and 32 granulosa shells. The results of the amiloride and the 10 μM cariporide + 1 μM S3226 co-treatment experiments have been added as a bar graph for ease of comparison.

V-ATPase (Drose and Altendorf, 1997). Bafilomycin dramatically inhibited the Na<sup>+</sup>-independent recovery (Fig. 5A,B; rate of recovery 0.005 ± 0.001 pHU/minute; *P* < 0.01), similar to NEM. Concanamycin

caused a partial inhibition (rate 0.013 ± 0.001 pHU/minute). Importantly, re-addition of Na<sup>+</sup> triggered a robust pH<sub>i</sub> increase in the presence of either antibiotic (Fig. 5A). We therefore conclude that

the  $\text{Na}^+$ - and  $\text{HCO}_3^-$ -independent  $\text{pH}_i$  increases observed in granulosa cells following induction of acidosis are attributable to a  $\text{H}^+$ -transporting V-ATPase.

### Gap junctions may provide follicle-enclosed oocytes with access to mechanisms that correct acidosis

Having characterized the mechanisms that drive acidosis recovery in granulosa cells, it was now important to determine whether the small growing oocyte, which by itself is incapable of recovering from acidosis, can access these mechanisms. To do this,  $\text{pH}_i$  was measured in small (40–60  $\mu\text{m}$  diameter) denuded and follicle-enclosed oocytes by microinjecting a cohort of each with SNARF-

dextran (10 kDa). Using this approach, the  $\text{pH}_i$  of follicle-enclosed oocytes can be monitored in the absence of contaminating fluorescence from the follicle cells, allowing simultaneous comparison with denuded oocytes (see Fig. 6). The initial 'resting'  $\text{pH}$  of follicle-enclosed oocytes ( $7.26 \pm 0.03$ ) was significantly higher than that of denuded counterparts ( $7.02 \pm 0.02$ ;  $P < 0.01$ ). Little or no recovery from acidosis occurred following  $\text{NH}_4\text{Cl}$  treatment in denuded oocytes, as in previous experiments ( $0.005 \pm 0.001$   $\text{pHU/minute}$ ). However,  $\text{pH}_i$  increased substantially in follicle-enclosed oocytes upon re-addition of  $\text{Na}^+$  (initial rate  $0.038 \pm 0.005$   $\text{pHU/minute}$ ), indicating that the granulosa cells afford the oocyte the capacity to recover from acidosis (Fig. 6A).

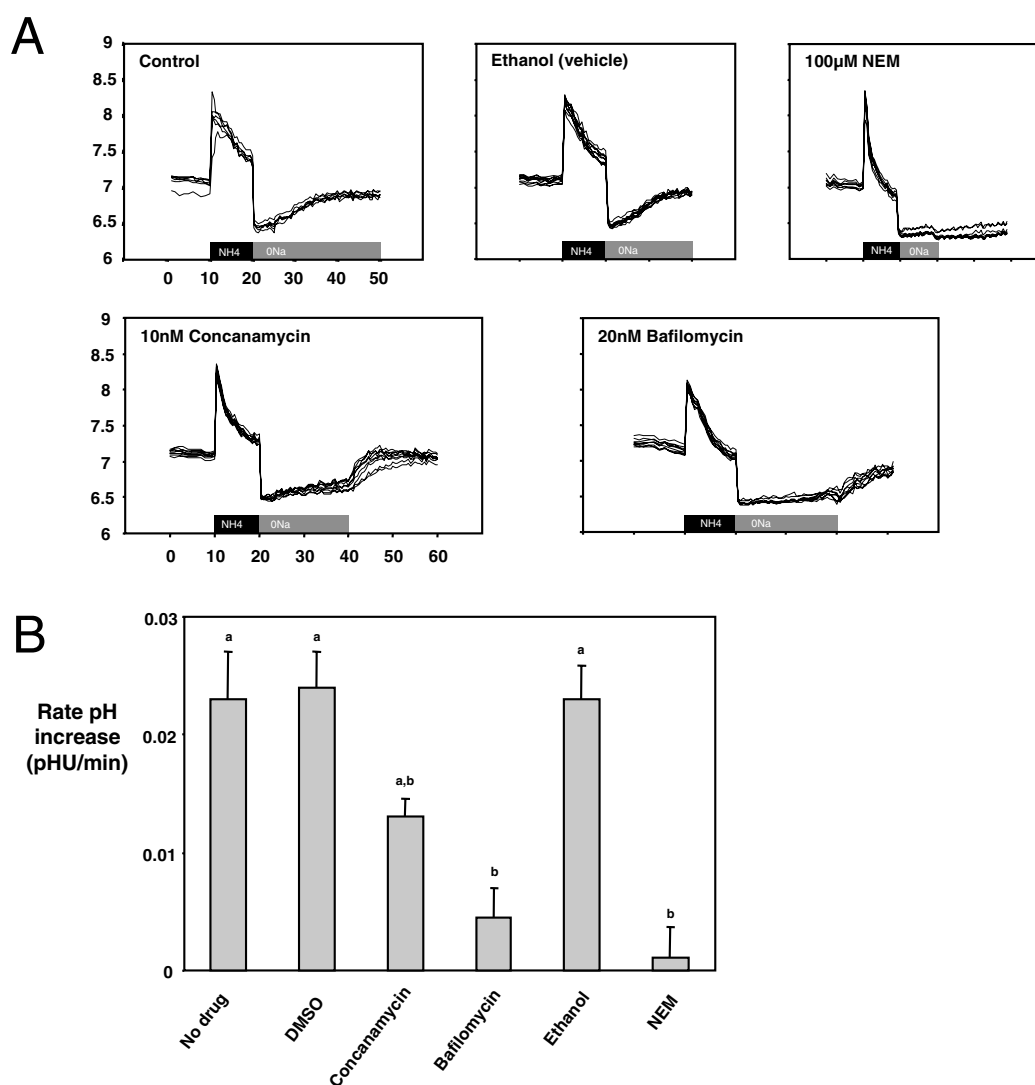


**Fig. 5. Investigation of  $\text{Na}^+$ -independent  $\text{pH}$  increases in granulosa cells.** Granulosa cells were acidified by  $\text{NH}_4\text{Cl}$  pulse in bicarbonate-free medium and  $\text{Na}^+$ -independent recovery examined. **(A)** Typical examples of each treatment group. Note that in control experiments, acidosis is almost fully relieved despite the absence of  $\text{Na}^+$ . Drugs or vehicles were added to the bath at  $t=10$  minutes, and remained throughout the experiment. NEM (100  $\mu\text{M}$ ) and bafilomycin (20 nM or 200 nM) retarded the  $\text{Na}^+$ -independent alkalinization that occurs following  $\text{NH}_4\text{Cl}$  removal in controls. A lower level of NEM (10  $\mu\text{M}$ ) partially inhibited recovery, whereas a higher level (1000  $\mu\text{M}$ ) did not further inhibit recovery (not shown). Bafilomycin was maximally effective at both 20 and 200 nM, and these data were combined (three replicates: one of 200 nM and two of 20 nM; due to the high cost of bafilomycin and the large volumes required for these experiments, the data for 20 and 200 nM were combined to yield three replicates). Concanamycin (10 nM) caused partial inhibition, which was not increased at 100 nM (not shown). **(B)** Summary of  $\text{Na}^+$ -independent acidosis correction. Each bar represents mean  $\pm$  s.d. of the initial rate of  $\text{pH}$  recovery from three replicates. Different letters indicate  $P < 0.01$  (ANOVA).



To establish whether gap junctions are involved in this, 18 $\alpha$ -glycyrrhetic acid (AGA), a small-molecule gap junction inhibitor, was employed. We have previously shown that a 10-

minute incubation with AGA completely inhibits oocyte-granulosa cytoplasmic continuity as determined by transfer of a fluorescent dye (FitzHarris and Baltz, 2006). Here, AGA

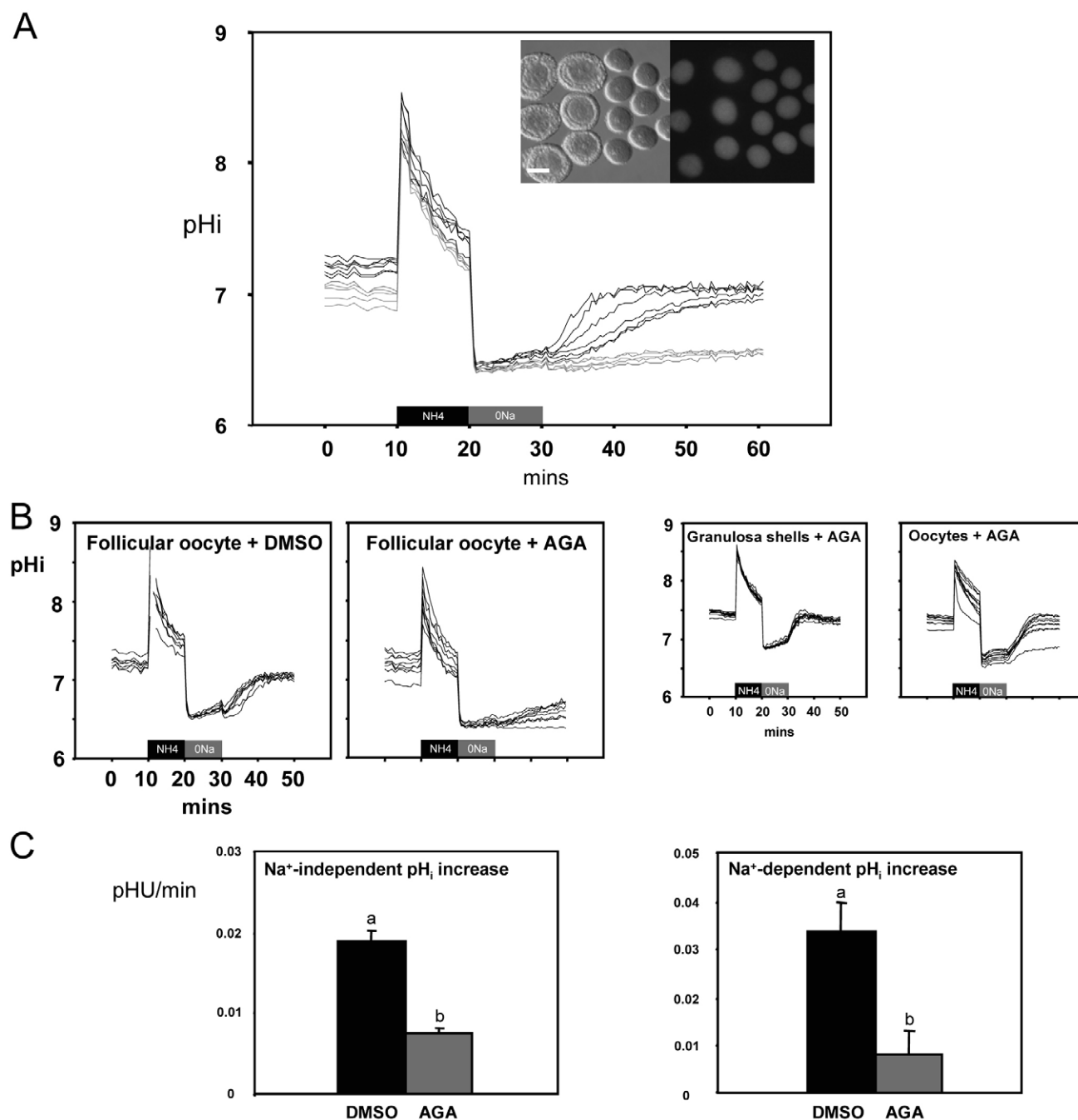


**Fig. 6. Gap junctions provide follicle-enclosed oocytes with access to mechanisms that correct acidosis.** SNARF-dextran was microinjected into denuded and follicle-enclosed oocytes from day-10 mice. **(A)** Recovery from acidosis was examined simultaneously in denuded and follicle-enclosed oocytes from day-10 mice using SNARF-dextran in bicarbonate-free medium. The graph shows a representative replicate of this experiment, in which six follicle-enclosed (black traces) and five denuded oocytes were examined. The follicle-enclosed oocytes recover from acidosis when Na<sup>+</sup> is replaced. The average rate of recovery following Na<sup>+</sup>-replacement is significantly greater in the follicle-enclosed oocytes over the course of three replicates ( $P < 0.05$ ). Note that the SNARF-dextran remains restricted to the oocyte within the follicle (inset). **(B)** Recovery from acidosis was examined in follicle-enclosed oocytes in the presence of DMSO (left panel) or 150  $\mu$ M AGA (centre), which were added during the experiment at  $t = 20$  minutes. A representative replicate of each treatment group is shown. **(C)** Analyses of the rate of pH recovery during the Na<sup>+</sup>-free period and following Na<sup>+</sup> replacement are shown. Each bar represents the mean of three separate replicates, a total of 19–29 follicle-enclosed oocytes. Different letters above bars indicate significant differences (ANOVA,  $P < 0.01$ ). Note that gap-junction inhibition abrogates both Na<sup>+</sup>-dependent and Na<sup>+</sup>-independent phases of acidosis recovery in follicle-enclosed oocytes. Note also that AGA does not inhibit acidosis recovery in fully grown oocytes, or shells of granulosa cells (B, right, one of two similar experiments is shown for each).

significantly inhibited the  $\text{Na}^+$ -dependent acidosis recovery (identified above as due to  $\text{Na}^+/\text{H}^+$  exchanger activity) in follicle-enclosed oocytes compared to controls ( $P < 0.01$ ; Fig. 6B,C). Moreover,  $\text{pH}_i$  increased steadily during the  $\text{Na}^+$ -free period in control (vehicle) follicle-enclosed oocytes ( $0.0189 \pm 0.001$  pHU/minute), and this  $\text{Na}^+$ -independent pH increase (identified above as due to V-ATPase activity) was also significantly inhibited by AGA ( $0.0074 \pm 0.001$  pHU/minute;  $P < 0.01$ ; Fig. 6C). AGA did not inhibit acidosis recovery in granulosa shells, or denuded fully grown germinal vesicle-stage oocytes, indicating that the ability of AGA to block acidosis recovery in follicle-enclosed growing oocytes is unlikely to be due to an unexpected effect on  $\text{pH}_i$  regulation (Fig. 6B, right). Thus, whereas small denuded oocytes are unable to recover from acidosis, follicle-enclosed oocytes possess acidosis-correcting activities that resemble those in the granulosa cells, provided gap junctions remain functional.

We also used octanol, another compound commonly employed as a gap junction inhibitor. Like AGA, octanol also eliminated the ability of follicle-enclosed oocytes to recover from acidosis, eliminating both the  $\text{Na}^+$ -dependent and  $\text{Na}^+$ -independent components. However, we found that octanol also inhibited the  $\text{Na}^+$ -dependent component of acidosis recovery in isolated granulosa shells to a varying extent, although the  $\text{Na}^+$ -independent component was unaffected. Therefore, whereas the experiments with octanol (not shown) were consistent with the conclusion that the enclosed oocyte  $\text{pH}_i$  is regulated by the surrounding granulosa cells, since the  $\text{Na}^+$ -independent (V-ATPase-dependent) recovery was not affected by octanol in granulosa shells but was eliminated in the enclosed oocyte, the apparent direct inhibition of  $\text{Na}^+/\text{H}^+$  exchange by octanol in granulosa cells precluded its use in examining the  $\text{Na}^+$ -dependent recovery.

### Simultaneous measurement of $\text{pH}_i$ in oocytes and granulosa cells

The most reasonable interpretation of the experiments presented hitherto is that gap junctions allow oocytes access to acidosis-correcting mechanisms within the granulosa cells. Within such a model we would predict that, in intact oocyte-granulosa complexes, recovery from acidosis should take place at least as quickly in granulosa cells as in the oocyte. To examine this directly, it was necessary to simultaneously monitor recovery from acidosis in oocytes and their surrounding granulosa cells, which we have done previously using partly denuded oocytes (FitzHarris and Baltz, 2006). Since it was not technically possible to obtain partly denuded oocytes from growing follicles, we instead used fully grown GV oocytes from PMSG-primed adult mice. Part-enclosed oocytes and their accompanying cumulus granulosa cells adopted a markedly higher  $\text{pH}_i$  than denuded oocytes, consistent with previous data (FitzHarris and Baltz, 2006). Recovery from acidosis occurred more rapidly in partly-enclosed oocytes. Strikingly, the  $\text{Na}^+$ -independent phase of recovery from acidosis, which we characterized in granulosa cells and follicle-enclosed oocytes, was evident in oocytes and accompanying granulosa cells in these experiments such that oocytes and accompanying granulosa recovered synchronously ( $0.018 \pm 0.005$  pHU/minute), whereas  $\text{pH}_i$  increase in  $\text{Na}^+$ -free medium in denuded oocytes imaged simultaneously was minimal ( $0.007 \pm 0.003$  pHU/minute;  $P < 0.05$ ; Fig. 7). In addition,  $\text{pH}_i$  recovery following  $\text{Na}^+$  replacement occurred more rapidly in partly enclosed oocytes in each experiment. These data are consistent with the other experiments presented here, indicating that oocytes have access to the acidosis-correcting mechanisms of the granulosa cells. In addition, this confirms that both the  $\text{Na}^+$ -dependent and -independent phases of recovery continue to be present in granulosa cells even when the oocyte is fully grown.

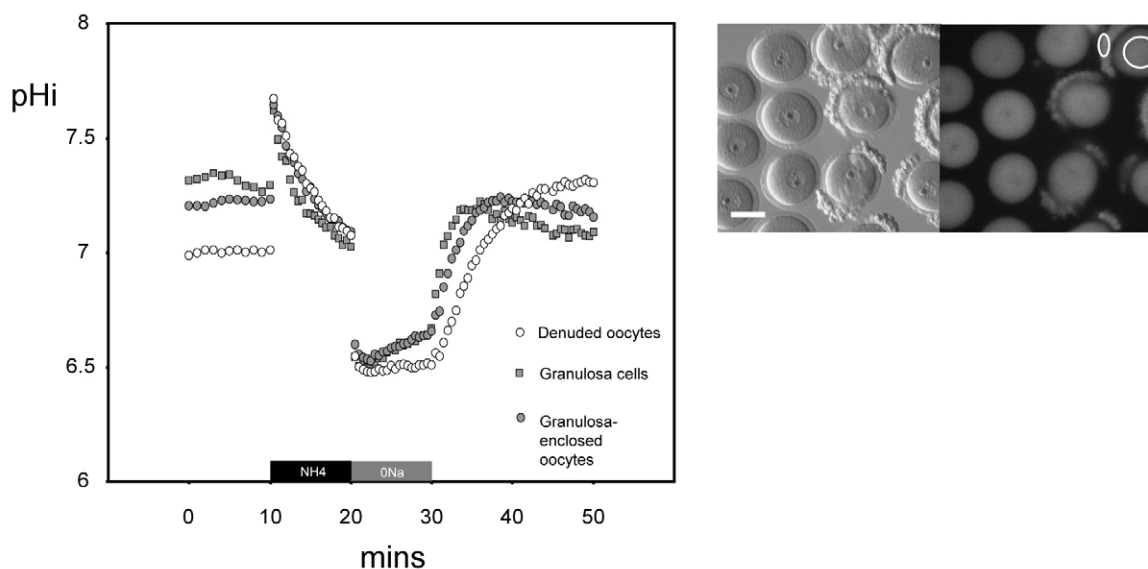


**Fig. 7. Synchronous recovery from acidosis in oocytes and accompanying granulosa cells.** Cumulus oocyte complexes from the ovaries of PMSG-primed adult mice were carefully cleaned so as to produce denuded oocytes, and oocytes with a part-covering of granulosa cells. Following loading with SNARF-AM, both oocyte and granulosa cell regions are clearly visible, such that regions of interest (ROI) for analysis can be positioned to measure pH independently in the different compartments (see inset; ROI examples outlined in white). The graph shown is one of four independent replicates, which comprised 26 denuded and 30 part-enclosed oocytes in total. The average curve for each cell type is shown. Note that  $\text{pH}_i$  of part-enclosed oocytes closely reflects that of the accompanying granulosa cells, including a steady  $\text{pH}_i$  increase which occurs during the  $\text{Na}^+$ -free period, which is not evident in denuded oocytes. Over the course of three experiments, 26 oocyte-granulosa complexes and 30 denuded oocytes were examined.

## DISCUSSION

The major finding here is that growing oocytes require granulosa cells and functional granulosa-oocyte gap junctions to correct acidosis. Fully grown denuded oocytes recover from an induced acidosis, but smaller oocytes lack this ability. When taken together with the previous finding that denuded small growing oocytes are incapable of correcting alkaline loads (Erdogan et al., 2005), this establishes the growing oocyte as a rare example of a mammalian cell unable to regulate its own  $pH_i$ . However, in the more physiological situation where the small oocyte is coupled to its granulosa cells, the  $pH_i$  of the oocyte can be maintained. The finding that small oocytes are only capable of raising their  $pH_i$  when coupled to granulosa cells explains the finding that small oocytes adopt a lower 'resting' pH when denuded (FitzHarris and Baltz, 2006) (Fig. 6). The low  $pH_i$  probably reflects the effect of electrochemical equilibrium or metabolic  $H^+$  generation on oocyte  $pH_i$  in the absence of  $pH_i$ -regulatory mechanisms and, as such, should be considered an artifact of removal from the ovary. As the oocyte grows it acquires the ability to regulate against acid loads, such that fully grown oocytes are capable of independently maintaining the appropriate  $pH_i$  when oocyte-granulosa gap junction communication is broken after ovulation is triggered.

## Distinct pH regulatory mechanisms in oocytes and granulosa cells

Using isoform-specific inhibitors, we were able to establish that oocytes acquire the ability to regulate against acidosis independently of granulosa cells by developing NHE1-mediated  $Na^+/H^+$  exchange activity. An examination of  $pH_i$  regulatory mechanisms was also carried out on granulosa cells from 10-day-old mice, at which stage the oocyte relies upon the granulosa cells for  $pH_i$  regulation. Granulosa cells were found to possess several distinct mechanisms. Robust  $Na^+/H^+$  exchange was only inhibited by treatments that simultaneously inactivated NHE1 and NHE3. These data imply that either isoform on its own is capable of driving maximal recovery from induced acidosis, indicating a functional redundancy between the two isoforms in granulosa cells. Two populations of distinctly regulated antiporters may also allow precise  $pH_i$  regulation during folliculogenesis. Consistent with the idea that NHE1 and NHE3 together account for  $Na^+$ -dependent,  $HCO_3^-$ -independent  $pH_i$  regulatory capacity in granulosa cells, *NHE1* and *NHE3* mRNAs were the only isoforms detected in granulosa cells by RT-PCR. The finding that a small proportion of  $Na^+$ -dependent recovery was amiloride-insensitive in  $HCO_3^-$ -containing, but not  $HCO_3^-$ -free,

medium, suggests that granulosa cells may also possess a minor component of  $Na^+$ ,  $HCO_3^-/Cl^-$  exchange, however, we have not investigated this further. An additional component of acidosis recovery was present in granulosa cells, which was  $HCO_3^-$  and  $Na^+$  independent, uninhibited by  $Na^+/H^+$  exchange inhibitors, and inhibited by bafilomycin, concanamycin and NEM, indicative of a V-type  $H^+$  ATPase. It is difficult to predict to what degree the V-ATPase contributes to  $pH_i$  homeostasis in vivo, as this component was less evident in  $HCO_3^-$ -containing medium, most likely masked by  $HCO_3^-/CO_2$ -based cytoplasmic buffering. Nonetheless, murine granulosa cells should be added to the relatively limited list of cells in which V-type  $H^+$  ATPases have been shown capable of regulating cytoplasmic  $pH_i$  (Nelson and Harvey, 1999; Merzendorfer et al., 1997; Kawasaki-Nishi et al., 2003). Avian granulosa cells possess an unidentified  $Na^+$ - and  $HCO_3^-$ -independent means of raising  $pH_i$  (Li et al., 1992), suggesting that plasmalemmal V-ATPase-mediated  $pH_i$  regulation may be conserved in granulosa cells. Overall, it is clear that granulosa cells have been amply equipped with mechanisms that regulate against  $pH_i$  changes, reflecting their unique role as the regulators of ooplasmic pH.

## Growing oocytes have access to granulosa cell $pH_i$ regulation

The current data strongly support a model in which gap junctions allow  $pH_i$ -regulatory mechanisms within granulosa cells to regulate oocyte  $pH_i$ . Strikingly, both the  $Na^+$ -dependent (NHE) and  $Na^+$ -independent (V-ATPase) phases of acidosis recovery evident in granulosa shells were echoed by granulosa-enclosed oocytes, and both were abrogated by gap-junction inhibition. The appearance of the  $Na^+$ -independent phase in follicle-enclosed oocytes is compelling, as we found no evidence that the oocyte itself ever exhibits  $pH_i$ -regulatory V-ATPase activity. Unfortunately, the presence of NHE1 in granulosa cells and denuded oocytes prevented us from selectively inhibiting granulosa cell  $Na^+/H^+$  exchange in intact follicles without affecting the  $Na^+/H^+$  exchange present in fully grown oocytes, an experiment which might have added evidence for the direct action of granulosa cell exchangers upon ooplasm  $pH_i$ . Nevertheless, we have been unable to prevent recovery from acidosis in follicle-enclosed oocytes using even 10  $\mu M$  cariporide (data not shown), a result which would not be expected if the function of the granulosa cells were to activate oocyte transporters, since  $Na^+/H^+$  exchange in fully grown oocytes was potentially inhibited by 1  $\mu M$  cariporide (see Fig. 2). Taken together, the evidence suggests that gap junctions allow the granulosa cells to

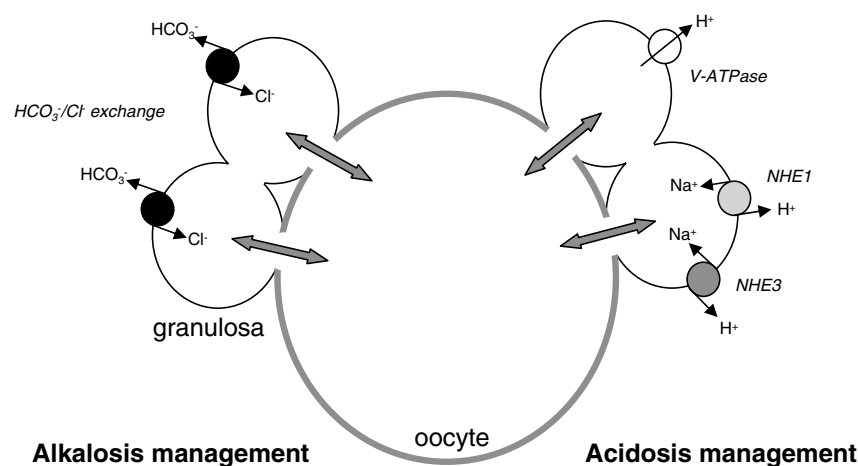


**Fig. 8. Model summarizing regulation of ooplasmic  $pH_i$  by granulosa cell transport mechanisms.** The small growing oocyte is incapable of regulating its own  $pH_i$ , but the gap junctions, which couple the oocyte and granulosa, allow exchangers on the granulosa cell surface to regulate the ooplasm. Granulosa cell exchangers that participate are indicated:  $Na^+/H^+$  exchanger isoform 1 (light gray circles), isoform 3 (dark gray), and V-ATPase (open circle). The molecular identity of the  $HCO_3^-/Cl^-$  exchangers that regulate against alkalosis is unknown (black circles). The broad arrows indicate diffusion of proton equivalents between oocyte and granulosa (see text).

serve as an extension of the oolemma, regulating ooplasmic  $\text{pH}_i$  on its behalf. Therefore the ovarian follicle provides the first demonstration that gap junctions can allow one cell to regulate the  $\text{pH}_i$  of its neighbour in a physiological setting, a notion that is summarised in Fig. 8. Though the identity of the molecules that traverse the gap junctions allowing  $\text{pH}_i$  to equilibrate between the oocyte and the granulosa cells is unknown, direct transfer of free protons is unlikely given the high buffering capacity of the cytoplasm (Swietach et al., 2003). Based on the rate of transfer of injected acid between gap junction-coupled cardiomyocytes it has been proposed that the mobile buffer should be around 200 Da, in which case taurine, inorganic phosphate, or dipeptides could be candidates (Zaniboni et al., 2003), and bicarbonate could also contribute under physiological conditions.

### $\text{pH}_i$ regulation during oocyte growth

To conclude, the growing mammalian oocyte is incapable of regulating its own  $\text{pH}_i$ , and has 'outsourced' this function to the granulosa cells, though the physiological benefit of this arrangement remains to be determined. Although  $\text{Na}^+/\text{H}^+$  and  $\text{HCO}_3^-/\text{Cl}^-$  exchange are passive secondary transporters, ATP hydrolysis is indirectly required to establish necessary transplasmalemmal ionic gradients. It may be that, during oocyte growth, energy resources are instead reserved for the metabolically expensive process of cell growth, or that reduced demands upon oocyte metabolism minimises potentially damaging effects of free radical production during the prolonged (tens of years in humans) meiotic arrest prior to recruitment into the growth phase.

This work was funded by a Canadian Institutes of Health Research Operating Grant (MOP74515) to J.M.B., and a CIHR Fellowship to G.F. The authors wish to thank Guillaume Halet and John Carroll for critical reading of the manuscript. We thank Dr Jürgen Pünter (Sanofi Aventis, Frankfurt) for the kind gifts of cariporide and S3226.

### References

- Ackert, C. L., Gittens, J. E., O'Brien, M. J., Eppig, J. J. and Kidder, G. M. (2001). Intercellular communication via connexin43 gap junctions is required for ovarian folliculogenesis in the mouse. *Dev. Biol.* **233**, 258-270.
- Alper, S. L. (1994). The band 3-related AE anion exchanger gene family. *Cell. Physiol. Biochem.* **4**, 265-281.
- Anderson, E. and Albertini, D. F. (1976). Gap junctions between the oocyte and companion follicle cells in the mammalian ovary. *J. Cell Biol.* **71**, 680-686.
- Baltz, J. M. and Phillips, K. P. (1999). Intracellular ion measurements in single eggs and embryos using ion-sensitive fluorophores. In *A Comparative Methods Approach to the Study of Oocytes and Embryos* (ed. J. D. Richter), pp. 39-82. New York, Oxford: Oxford University Press.
- Biggers, J. D., Whittingham, D. G. and Donahue, R. P. (1967). The pattern of energy metabolism in the mouse oocyte and zygote. *Proc. Natl. Acad. Sci. U.S.A.* **58**, 560-567.
- Bowman, E. J., Siebers, A. and Altendorf, K. (1988). Bafilomycins: a class of inhibitors of membrane ATPases from microorganisms, animal cells, and plant cells. *Proc. Natl. Acad. Sci. U.S.A.* **85**, 7972-7976.
- Brower, P. T. and Schultz, R. M. (1982). Intercellular communication between granulosa cells and mouse oocytes: existence and possible nutritional role during oocyte growth. *Dev. Biol.* **90**, 144-153.
- Buccione, R., Vanderhyden, B. C., Caron, P. J. and Eppig, J. J. (1990). FSH-induced expansion of the mouse cumulus oophorus in vitro is dependent upon a specific factor(s) secreted by the oocyte. *Dev. Biol.* **138**, 16-25.
- Colonna, R. and Mangia, F. (1983). Mechanisms of amino acid uptake in cumulus-enclosed mouse oocytes. *Biol. Reprod.* **28**, 797-803.
- Cross, P. C. and Brinster, R. L. (1974). Leucine uptake and incorporation at three stages of mouse oocyte maturation. *Exp. Cell Res.* **86**, 43-46.
- Drose, S. and Altendorf, K. (1997). Bafilomycins and concanamycins as inhibitors of V-ATPases and P-ATPases. *J. Exp. Biol.* **200**, 1-8.
- Ducibella, T., Albertini, D. F., Anderson, E. and Biggers, J. D. (1975). The preimplantation mammalian embryo: characterization of intercellular junctions and their appearance during development. *Dev. Biol.* **45**, 231-250.
- Erdogan, S., FitzHarris, G., Tartia, A. P. and Baltz, J. M. (2005). Mechanisms regulating intracellular pH are activated during growth of the mouse oocyte coincident with acquisition of meiotic competence. *Dev. Biol.* **286**, 352-360.
- Eppig, J. J. (1977). Mouse oocyte development in vitro with various culture systems. *Dev. Biol.* **60**, 371-388.
- Eppig, J. J. (1979). A comparison between oocyte growth in coculture with granulosa cells and oocytes with granulosa cell-oocyte junctional contact maintained in vitro. *J. Exp. Zool.* **209**, 345-353.
- Eppig, J. J. (1991). Mammalian oocyte development in vivo and in vitro. In *Elements of Mammalian Fertilization, Volume I: Basic Concepts* (ed. P. M. Wassarman), pp. 57-76. Boca Raton: CRC Press.
- Eppig, J. J. and Wigglesworth, K. (2000). Development of mouse and rat oocytes in chimeric reaggregated ovaries after interspecific exchange of somatic and germ cell components. *Biol. Reprod.* **63**, 1014-1023.
- FitzHarris, G. and Baltz, J. M. (2006). Granulosa cells regulate intracellular pH of the murine growing oocyte via gap junctions: development of independent homeostasis during oocyte growth. *Development* **133**, 591-599.
- Grinstein, S., Rotin, D. and Mason, M. J. (1989).  $\text{Na}^+/\text{H}^+$  exchange and growth factor-induced cytosolic pH changes. Role in cellular proliferation. *Biochim. Biophys. Acta* **988**, 73-97.
- Haghighat, N. and van Winkle, L. J. (1990). Developmental change in follicular cell-enhanced amino acid uptake into mouse oocytes that depends on intact gap junctions and transport system Gly. *J. Exp. Zool.* **253**, 71-82.
- Harding, E. A., Gibb, C. A., Johnson, M. H., Cook, D. I. and Day, M. L. (2002). Developmental changes in the management of acid loads during preimplantation mouse development. *Biol. Reprod.* **67**, 1419-1429.
- Heller, D. T. and Schultz, R. M. (1980). Ribonucleoside metabolism by mouse oocytes: metabolic cooperativity between the fully grown oocyte and cumulus cells. *J. Exp. Zool.* **214**, 355-364.
- Heller, D. T., Cahil, D. M. and Schultz, R. M. (1981). Biochemical studies of mammalian oogenesis: metabolic cooperativity between granulosa cells and growing mouse oocytes. *Dev. Biol.* **84**, 455-464.
- Kapus, A., Grinstein, S., Wasan, S., Kandasamy, R. and Orlowski, J. (1994). Functional characterization of three isoforms of the  $\text{Na}^+/\text{H}^+$  exchanger stably expressed in Chinese hamster ovary cells. ATP dependence, osmotic sensitivity, and role in cell proliferation. *J. Biol. Chem.* **269**, 23544-23552.
- Kawagishi, R., Tahara, M., Sawada, K., Morishige, K., Sakata, M., Tasaka, K. and Murata, Y. (2004).  $\text{Na}^+/\text{H}^+$  exchanger-3 is involved in mouse blastocyst formation. *J. Exp. Zool.* **301**, 767-775.
- Kawasaki-Nishi, S., Nishi, T. and Forgac, M. (2003). Proton translocation driven by ATP hydrolysis in V-ATPases. *FEBS Lett.* **545**, 76-85.
- Kidder, G. M. and Mhaw, A. A. (2002). Gap junctions and ovarian folliculogenesis. *Reproduction* **123**, 613-620.
- Lane, M., Baltz, J. M. and Bavister, B. D. (1998). Regulation of intracellular pH in hamster preimplantation embryos by the sodium hydrogen ( $\text{Na}^+/\text{H}^+$ ) antiporter. *Biol. Reprod.* **59**, 1483-1490.
- Lawitts, J. A. and Biggers, J. D. (1993). Culture of preimplantation embryos. *Meth. Enzymol.* **225**, 153-164.
- Li, M., Morley, P., Schwartz, J. L., Whitfield, J. F. and Tsang, B. K. (1992). Muscarinic cholinergic stimulation elevates intracellular pH in chicken granulosa cells by a  $\text{Ca}^{2+}$ -dependent,  $\text{Na}^+$ -independent mechanism. *Endocrinology* **131**, 235-239.
- Masereel, B., Pochet, L. and Laeckmann, D. (2003). An overview of inhibitors of  $\text{Na}^+/\text{H}^+$  exchanger. *Eur. J. Med. Chem.* **38**, 547-554.
- Merzendorfer, H., Graf, R., Huss, M., Harvey, W. R. and Wiczorek, H. (1997). Regulation of proton-translocating V-ATPases. *J. Exp. Biol.* **200**, 225-235.
- Nakamura, N., Tanaka, S., Teko, Y., Mitsui, K. and Kanazawa, H. (2005). Four  $\text{Na}^+/\text{H}^+$  exchanger isoforms are distributed to Golgi and post-Golgi compartments and are involved in organelle pH regulation. *J. Biol. Chem.* **280**, 1561-1572.
- Nelson, N. and Harvey, W. R. (1999). Vacuolar and plasma membrane proton-adenosinetriphosphatases. *Physiol. Rev.* **79**, 361-385.
- Orlowski, J. and Grinstein, S. (1997).  $\text{Na}^+/\text{H}^+$  exchangers of mammalian cells. *J. Biol. Chem.* **272**, 22373-22376.
- Orlowski, J. and Grinstein, S. (2004). Diversity of the mammalian sodium/proton exchanger SLC9 gene family. *Pflügers Arch.* **447**, 549-565.
- Phillips, K. P., Petrunewich, M. A. F., Collins, J. L. and Baltz, J. M. (2002). The intracellular pH-regulatory  $\text{HCO}_3^-/\text{Cl}^-$  exchanger in the mouse oocyte is inactivated during first meiotic metaphase and reactivated after egg activation via the MAP kinase pathway. *Mol. Biol. Cell* **13**, 3800-3810.
- Pouyssegur, J., Sardet, C., Franchi, A., L'Allemain, G. and Paris, S. (1984). A specific mutation abolishing  $\text{Na}^+/\text{H}^+$  antiport activity in hamster fibroblasts precludes growth at neutral and acidic pH. *Proc. Natl. Acad. Sci. USA* **81**, 4833-4837.
- Romero, M. F., Fulton, C. M. and Boron, W. F. (2004). The SLC4 family of  $\text{HCO}_3^-$  transporters. *Pflügers Arch.* **447**, 495-509.
- Schwark, J. R., Jansen, H. W., Lang, H. J., Krick, W., Burckhardt, G. and Hropot, M. (1998). S3226, a novel inhibitor of  $\text{Na}^+/\text{H}^+$  exchanger subtype 3 in various cell types. *Pflügers Arch.* **436**, 797-800.
- Simon, A. M., Goodenough, D. A., Li, E. and Paul, D. L. (1997). Female infertility in mice lacking connexin 37. *Nature* **385**, 525-529.



- Sorensen, R. A. and Wassarman, P. M.** (1976). Relationship between growth and meiotic maturation of the mouse oocyte. *Dev. Biol.* **50**, 531-536.
- Steeves, C. L., Lane, M., Bavister, B. D., Phillips, K. P. and Baltz, J. M.** (2001). Differences in intracellular pH regulation by Na<sup>+</sup>/H<sup>+</sup> antiporter among two-cell mouse embryos derived from females of different strains. *Biol. Reprod.* **65**, 14-22.
- Sternlicht, A. L. and Schultz, R. M.** (1981). Biochemical studies of mammalian oogenesis: kinetics of accumulation of total and poly(A)-containing RNA during growth of the mouse oocyte. *J. Exp. Zool.* **215**, 191-200.
- Swietach, P., Zaniboni, M., Stewart, A. K., Rossini, A., Spitzer, K. W. and Vaughan-Jones, R. D.** (2003). Modelling intracellular H<sup>+</sup> ion diffusion. *Prog. Biophys. Mol. Biol.* **83**, 69-100.
- Zaniboni, M., Rossini, A., Swietach, P., Banger, N., Spitzer, K. W. and Vaughan-Jones, R. D.** (2003). Proton permeation through the myocardial gap junction. *Circ. Res.* **93**, 726-35.
- Zhao, Y., Chauvet, P. J., Alper, S. L. and Baltz, J. M.** (1995). Expression and function of bicarbonate/chloride exchangers in the preimplantation mouse embryo. *J. Biol. Chem.* **270**, 24428-24434.